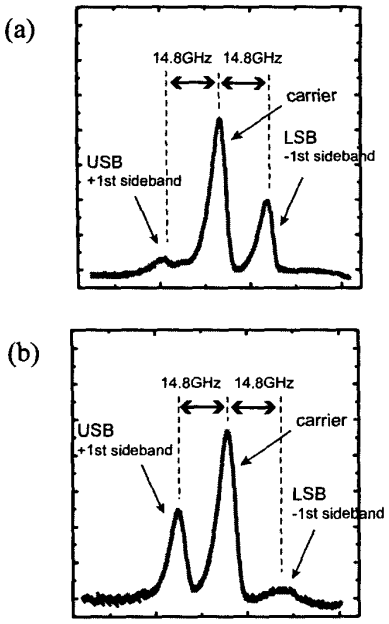

CTuK14 Fig. 2. Optical frequency spectra measured by using the scanning Fabry-Perot interferometer. The modulation frequency and the input power were 14.8 GHz and 25 dBm, respectively. The DC voltage was +12 V for (a) and −34 V for (b).

lated as ~6 GHz around the peak modulation frequency of 15 GHz for the total electrode length of 20.5 mm. The bandwidth can be enlarged as ~18 GHz by use of the non-periodically domain-inverted structure, which is shown in the Fig. 3 (b). Further improvements of the device for the enlargement of the bandwidth and the reduction of the driving microwave power and the DC voltage are now underway.

References

1. M. Izutsu, S. Shikama, T. Sueta, "Integrated optical SSB modulator/frequency shifter," *IEEE J. Quantum Electron.*, QE-17, 2225–2227 (1981).
2. G.H. Smith, D. Novak, Z. Ahmed, "Technique for optical SSB generation to overcome dispersion penalties in fiber-radio systems," *Electron. Lett.*, 33, 74–75 (1997).
3. S. Shimotsu, S. Oikawa, T. Saitou, N. Mitsugi, K. Kubodera, T. Kawanishi, M. Izutsu, "Single side-band modulation performance of a $LiNbO_3$ integrated modulator consisting of four-phase modulator waveguides," *IEEE Photon. Technol. Lett.*, 13, 364–366 (2001).
4. H. Murata, K. Kinoshita, G. Miyaji, A. Morimoto, and T. Kobayashi, "Quasi-velocity-matched $LiTaO_3$ guided-wave optical phase modulator for integrated ultrashort optical pulse generators," *Electron. Lett.*, 36, 1459–1460 (2000).
5. H. Murata, A. Morimoto, T. Kobayashi, and S. Yamamoto, "Optical pulse generation by electrooptic modulation method and its application to integrated ultrashort pulse generators," *IEEE J. Selected Topics Quantum Electron.*, 6, 1325–1331 (2000).

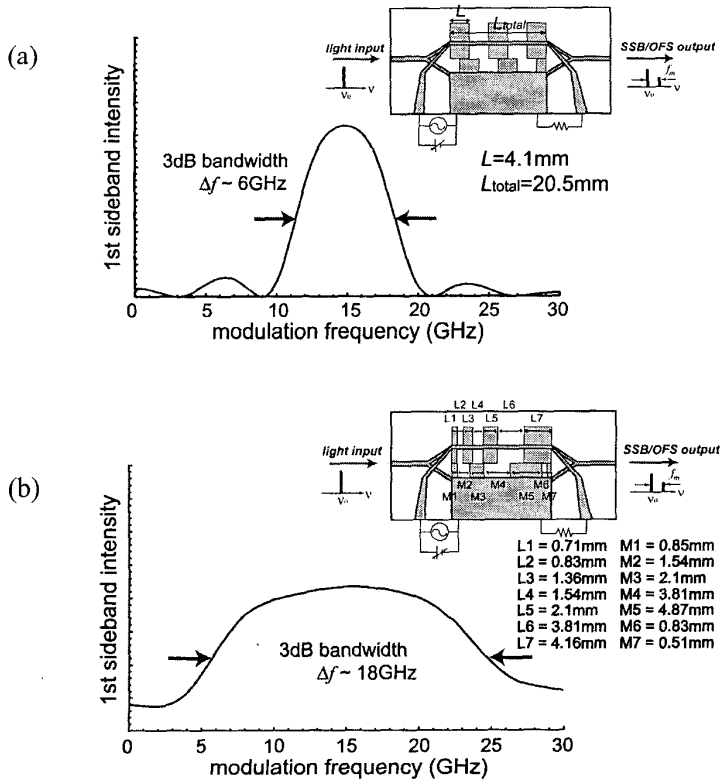

CTuK14 Fig. 3. Calculated frequency dependences of the SSB modulators with the periodic (a) and the non-periodic (b) domain-inversion schemes.

CTuK15 **1:00 pm**

Ge Quantum Dots Sandwiched between Two Thick Si Blocking Layers to Increase High Detectivity

Y.H. Peng, C.C. Chen, and C.H. Kuan, Department of Electrical Engineering, and Graduate Institute of Electronics Engineering, National Taiwan University, Taipei, Taiwan

H.H. Cheng Center for Condensed Matter Sciences, National Taiwan University, Taipei, Taiwan

In Fig. 1 are shown the voltage characteristics of the dark current (solid curves) and 300 K-background photocurrent (dash curve). Comparing these two currents, the background-limited performance can be observed at 50 K when the detector is operated under +0.33 V. The lower the operating temperature is, the higher the applied voltage is. For the dark current at low temperature, it is obvious that the current is divided into two regimes. One of them is dominated by the thermionic emission under low biases. The other is dominated by the thermally assisted tunneling under high bias.

The responsivity spectrum showed in Fig. 2 have its operative range from 2 to 10 μm under zero bias and will increase its magnitude and extend its range to 20 μm when the applied bias is increased. This property indicates the responsivity at zero bias is due to the hole transition between the ground and extended states in the QDs, while the long-wavelength one (10 ~ 20 μm) is due to the transition between the ground and bound states.

The detectivity in this sample at 30 K has maximum value toward 2.1×10^{10} cm $(Hz^{0.5})/W$ under 0.2 V for the 6 μm wavelength. The detectivity for the long wavelength is $\sim 10^9$ cm $(Hz^{0.5})/W$. It is also found in Fig. 3, there are two primary trends for the detectivity, which are consistent with the two mechanics in the responsivity. One trend shows a maximum detectivity, and the other increases monotonically with the applied bias. The separating wavelength is about 10 μm.

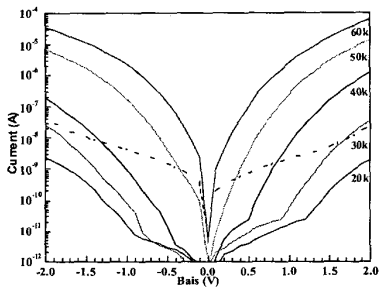

CTuK15 Fig. 1. The characteristics of the dark current from 20 K to 60 K and background photocurrent; the solid lines are dark current and the dash line is background photocurrent at 30 K.

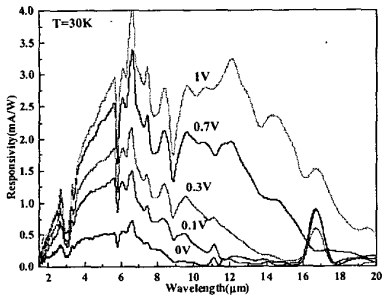

CTuK15 Fig. 2. The Responsivity spectrum under forward bias from 0V to 1V.

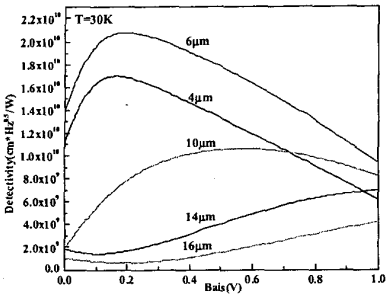

CTuK15 Fig. 3. The detectivity curves of various wavelengths under forward bias from 0V to 1V.

In summary, our Ge QDIP shows a satisfactory detectivity. The responsivity is active in the 2 ~ 10 μm under low biases and can be extended up to 20 um under high biases.

CTuK16 **1:00 pm**

Phase Conjugation by Degenerate Four-wave Mixing in a Solid-dye Laser

Hirofumi Watanabe, Takashige Omatsu, and Mitsuhiro Tateda, Department of Information and Image Sciences, Chiba University, 1-33, Yayoi-cho, Inage-Ku, Chiba 263-8522, Japan, Email:omatsu@image.tp.chiba-u.ac.jp

Phase conjugation by intra-cavity four-wave mixing (FWM) in laser media has been the subject of intense investigation, because of its high reflectivity.[1–5] Solid-dye lasers combine much of the convenience of solid state lasers with tunability and the high gain of a dye laser. Hence, the use of the solid-dye allows an efficient and compact solid-state phase conjugate mirror.

In this report, we present the first demonstration, to the best of our knowledge, of phase conjugation by four-wave mixing in a solid-dye laser itself. Since the laser itself is used as the nonlinear material, no additional nonlinear crystal is needed. In addition, the counter-propagating pump beams are automatically provided by laser oscillation. This system holds promise for applications of compact, easy to handle phase conjugation in the visible region. Experimental phase conjugate reflectivity of ~2% was obtained.

The scheme used is similar to the one described by Tomita, who used Nd:YAG [1] and Brignon, who used Nd:YVO_4.[3] In the scheme, the laser itself is used as a phase conjugate mirror, so that only one gain medium is required. The dye used was composed of a matrix of PMMA with less than 0.1-wt.% doping of Rhodamine 6G dye. Its dimensions were ϕ50 mm × 8 mm. We obtained population inversion by longitudinal laser pumping from both sides of the solid laser dye with a frequency-doubled Q-switched Nd:YAG laser. The combined external gain-pump beam fluence was 130–280 mJ/cm^2. The single-pass energy gain and the gain saturation fluence of the solid laser dye were estimated to be 74 and 1.3 mJ/cm^2, respectively.

A schematic diagram of the experimental setup for FWM in the solid dye laser is shown in Fig. 1. A laser cavity was formed by two mirrors (M_1, M_2) with reflectivies of 35% and >99%, respectively, for 570 nm and a grazing-incidence grating with 2400 lines/mm. A portion of the output beam reflected by the grating is used as a probe beam and, is injected back into the gain media by a concave mirror M_3 with reflectivity of 4% for 570 nm and a curvature radius of 400 mm. The counter-propagating pump beams are automatically provided by laser oscillation. Owing to the low coherence length (<1 cm) of the laser, the path length of the probe beam is adjusted to be the same as that between the M_3 and the gain media, thereby all beams interfere well. Without the grazing-incidence grating, phase conjugation could not be observed, because of too low coherence length of the laser.

Figure 2 shows the experimental phase conjugate reflectivity as a function of external gain-pump beam fluence. Measured phase conjugate reflectivity was typically 1–2% over the full external gain-pump fluence. This phenomenon is due to saturable absorption by the external gain-pump laser.

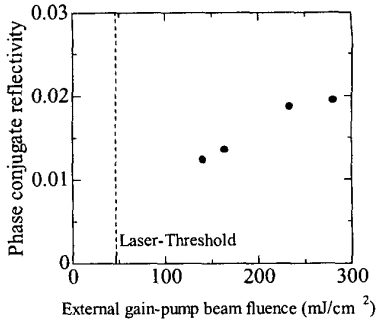

CTuK16 Fig. 2. Phase conjugate energy reflectivity with intra-cavity FWM versus external gain-pump beam fluence.

In conclusion, we have demonstrated the first demonstration of phase conjugation by degenerate four-wave mixing in a solid dye laser itself. Phase conjugate reflectivity of ~2% was obtained. This system should be useful for applications in dynamic holography, signal processing, and phase conjugation.

References

1. A. Tomita, "Phase conjugation using gain saturation of Nd:YAG laser," Appl. Phys. Lett. **34**, 463 (1979).
2. G.J. Crofts, R.P. Green, and M.J. Damzen, Opt. Lett. **17**, 920 (1992).
3. A. Brignon, L. Loiseau, C. Larat, J.-P. Huignard, and J.-P. Pocholle, "Phase conjugation in a continuous-wave diode-pumped Nd:YVO_4 laser," Appl. Phys. B, **69**, 159 (1999).
4. A. Brignon, G. Feugnet, J.-P. Huignard, and J.-P. Pocholle, "Efficient degenerate four-wave mixing in a diode-pumped microchip Nd:YVO_4 amplifier," Opt. Lett. **20**, 548 (1995).
5. H. Watanabe, T. Omatsu, T. Hirose, and M. Tateda, "Tunable phase conjugation by intracavity degenerate four-wave mixing in an injection-seeded solid dye laser," Opt. Lett. **25**, 1267 (2000).

coherence length of the laser.

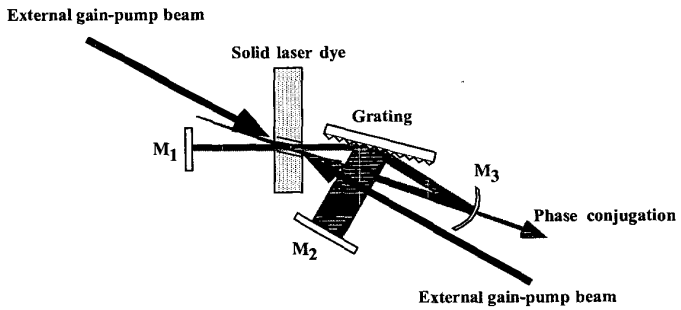

CTuK16 Fig. 1. Schematic diagram of the intra-cavity FWM in a solid dye laser.

CTuK17 **1:00 pm**

High Quality 7.5 Watt Output from a CW Nd:YVO_4 Photorefractive Phase Conjugate Resonator

T. Omatsu Department of Information and Image Sciences, Chiba University, 1-33, Yayoi-cho, Inage-ku, Chiba 263-8522, Japan, Email: omatsu@image.tp.chiba-u.ac.jp

A. Minassian, M.J. Damzen, Blackett Laboratory, Imperial College, Prince Consort Rd., London SW7 2BW, UK, Email: m.damzen@ic.ac.uk

Photorefractive phase conjugate resonators (PPCR), in which one end mirror is a self-pumped photorefractive phase conjugate mirror (PCM), have received an intense attention, because of its correction of thermal distortions in the laser resonator and laser oscillation without